JACS
JOURNAL OF THE AMERICAN CHEMICAL SOCIETY
Communication
pubs.acs.org/JACS

# Fullerene/Cobalt Porphyrin Hybrid Nanosheets with Ambipolar Charge Transporting Characteristics

Takatsugu Wakahara,*[,†,‡] Pasquale D'Angelo,[‡] Kun'ichi Miyazawa,[†] Yoshihiro Nemoto,[§] Osamu Ito,[†,#] Nobutaka Tanigaki,[∥] Donal D.C. Bradley,*[,‡] and Thomas D. Anthopoulos*[,‡]

[†]Fullerene Engineering Group, Advanced Materials Processing Unit, Advanced Key Technologies Division, National Institute for Materials Science, 1-1 Namiki, Tsukuba, Ibaraki 305-0044, Japan

[‡]Department of Physics and Centre for Plastic Electronics, Blackett Laboratory, Imperial College London, London SW7 2BW, U.K.

[§]ICYS, National Institute for Materials Science, 1-1 Namiki, Tsukuba, Ibaraki 305-0044, Japan

[#]CarbonPhotoScience Institute, Kita-Nakayama2-1-6, Izumi-ku, Sendai, 981-3215, Japan

[∥]Photonic Device Application Group, Research Institute for Ubiquitous Energy Devices, National Institute of Advanced Industrial Science and Technology, 1-18-31 Midorigaoka, Ikeda 563-8577, Japan

Supporting Information

**ABSTRACT:** A novel supramolecular nanoarchitecture, comprising $C_{60}$/Co porphyrin nanosheets, was prepared by a simple liquid−liquid interfacial precipitation method and fully characterized by means of optical microscopy, AFM, STEM, TEM, and XRD. It is established that the highly crystalline $C_{60}$/Co porphyrin nanosheets have a simple (1:1) stoichiometry, and when incorporated in bottom-gate, bottom-contact field-effect transistors (FETs), they show ambipolar charge transport characteristics.

Functional supramolecular nanoarchitectures have tremendous potential as building blocks of bottom-up organic nano- and micrometer-scale devices[1−3] such as transistors.[4] Recently, there have been many reports on transistors employing supramolecular nanoarchitectures such as nanowhiskers (NWs), nanotubes, nanorods, nanowires, and nanosheets.[1,5,6] A distinct characteristic of almost all these reported transistors is that they transport only a single carrier type, either holes (p-type) or electrons (n-type). Therefore, simultaneous or selectable transport of electrons and/or holes (ambipolar charge transport) remains a highly desirable characteristic to be achieved, because it could enable the design of better performing electronic circuits[7] as well as the demonstration of bifunctional organic devices such as light-emitting[8] and light-sensing transistors.[9] To date, very little work has been done to establish supramolecular nanoarchitectures with ambipolar transport properties. Very recently, Mativetsky et al. reported ambipolar transistors based on donor (D)−acceptor (A) dyad architectures.[10] The workers synthesized a new D−A dyad, based on HBC-PMI (hexabenzocorone−perylene monoimide) bridged through a linker, which forms self-assembled fibers. Aida et al. prepared chiral-porphrin−fullerene dyad based nanofiber which showed ambipolar charge-carrier transport probed by time-resolved microwave conductivity (TRMC) but not field-effect measurements.[11]

Among the various acceptor molecules reported to date, fullerenes are known to form a wide variety of D−A complexes with different classes of organic and organometallic donors.[12,13] These complexes show a diverse spectrum of physical properties, including metallic conductivity,[14] photoconductivity,[15] and unusual magnetic properties.[16] Within this family, we have recently reported the preparation of $C_{60}$/ferrocene (Fc) hybrid hexagonal nanosheets by a liquid−liquid interfacial precipitation (LLIP) method.[17]

In the area of donor molecules, porphyrins are very well know and represent an important class of organic compounds because they combine excellent light harvesting characteristics with strong electron-donating properties.[18] As a result, various supramolecular fullerene−porphyrin architectures have been reported.[19−22] Recently, such fullerene−porphyrin co-crystals were reported to show electron-only transport probed by TRMC measurements.[23,24]

We herein report the preparation of novel $C_{60}$/5,10,15,20-tetrakis(4-methoxyphenyl) porphyrinato cobalt(II) (CoTMPP) hybrid nanosheets using the LLIP method. With these $C_{60}$/CoTMPP hybrid nanosheets, we have fabricated bottom-gate, bottom-contact FETs. Despite the nonoptimized device architecture employed, we found that $C_{60}$/CoTMPP hybrid nanosheets based FETs exhibit ambipolar transport characteristics with nearly balanced hole−electron mobilities. We attribute this behavior to the incorporation of CoTMPP since transistors based on $C_{60}$ alone are usually unipolar n-type devices.[20,25,26]

The $C_{60}$/CoTMPP hybrid nanosheets were formed at an interface between isopropyl alcohol (IPA) and toluene. Specifically, 4 mL of $C_{60}$-saturated toluene was placed in a 15 mL glass bottle and 9 mg of CoTMPP was added to this solution. After 10-min ultrasonication at room temperature, the $C_{60}$/CoTMPP solution was cooled to 10 °C in a cooling bath. To the surface of this toluene solution, 8 mL of IPA was added slowly, and the mixture was maintained at 10 °C for 5 min without disturbing the interface. The resulting two-layer mixture was vigorously shaken and stored at 10 °C for 24 h

**Received:** December 22, 2011
**Published:** April 19, 2012





dx.doi.org/10.1021/ja211951v | J. Am. Chem. Soc. 2012, 134, 7204−7206

during which the growth of dark colored precipitates was observed.

Figure 1 shows optical microscope images of the prepared dark colored precipitates. These representative images show the

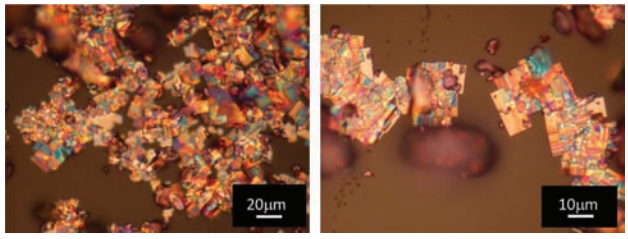


**Figure 1.** Optical microscopy images of nanosheets at different magnification.

tetragonal morphology of the precipitates with sizes in the range 5−10 $\mu$m and the tendency of the nanosheets to stack together. Figure 2 shows TEM and HR-TEM images of a single

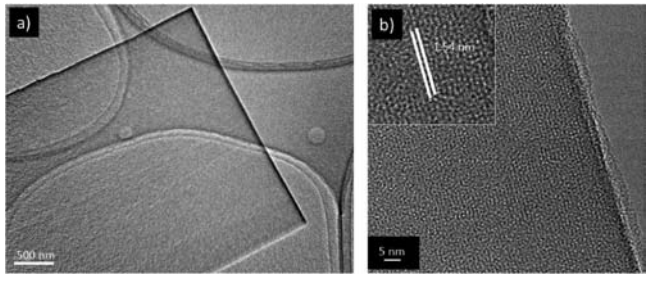


**Figure 2.** (a) TEM and (b) HRTEM images (inset: magnified image) of a single nanosheet.

tetragonal nanosheet, which appears as a highly transparent thin plate. A clear lattice structure is evident in the high-resolution image (Figure 2b) with spacing, *d*, calculated to be 1.54 nm. The thickness of the nanosheets, determined by AFM measurements, is ∼50−200 nm.

To spatially locate the CoTMPP molecules within the nanosheets, a STEM mapping analysis was carried out (Figure 3). Carbon and cobalt atoms were detected as shown in Figure

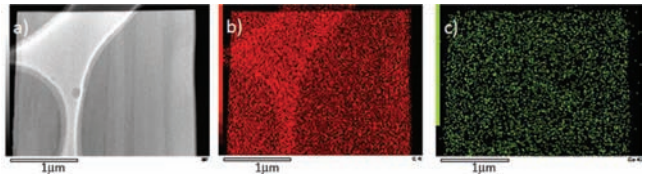


**Figure 3.** (a) STEM image of a $C_{60}$/CoTMPP nanosheet and (b, c) STEM mapping images (b: carbon; c: Cobalt) of $C_{60}$/CoTMPP nanosheet.

3, panels b and c, respectively. The distribution and concentration of carbon and cobalt atoms was found to be uniform across the whole nanosheet. This result confirms the fine dispersion of cobalt atoms in the nanosheets, indicating that the nanosheets comprise $C_{60}$/CoTMPP.

The crystal structure of the $C_{60}$/CoTMPP nanosheets was determined by X-ray diffraction (XRD) measurements. XRD patterns of the $C_{60}$ powder and $C_{60}$/CoTMPP nanosheets are shown in Figure 4. We observed two sets of XRD patterns. One originated from $C_{60}$/CoTMPP nanosheets and the other from

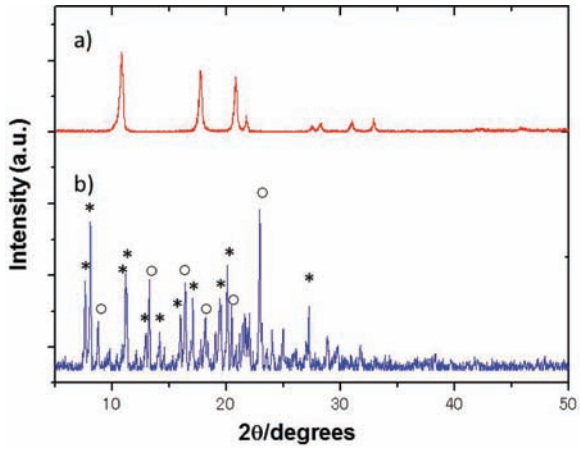


**Figure 4.** XRD patterns of (a) $C_{60}$ powder and (b) $C_{60}$/CoTMPP nanosheets. The peaks indicated by stars and open circles correspond to the CoTMPP·$C_{60}$ crystal and the CoTMPP powder.

the excess of CoTMPP. The XRD pattern of the $C_{60}$/CoTMPP nanosheets is quite different from that of the $C_{60}$ powder, but almost identical to that reported for CoTMPP·$C_{60}$(1:1) prepared in the presence of excess Fc.[27] It is noted that CoTMPP·2$C_{60}$·3(toluene) was reported to form in the absence of Fc.[27]

To investigate the charge transport properties of the $C_{60}$/CoTMPP nanosheets, we fabricated bottom-gate, bottom-contact FETs employing gold source-drain electrodes and $SiO_2$ as the gate dielectric. Figure 5 shows transfer ($I$−$V_G$)

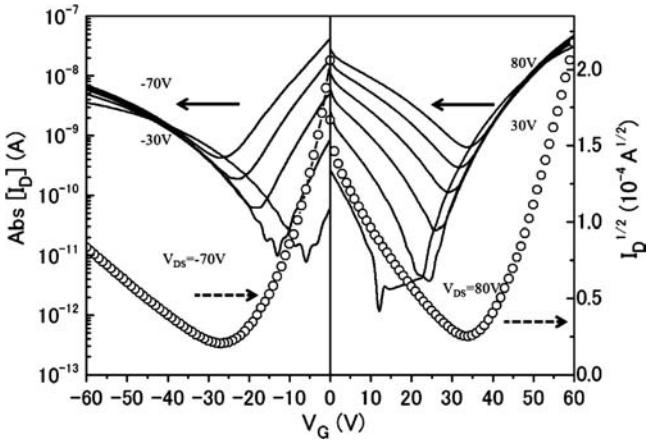


**Figure 5.** The transfer characteristics of $C_{60}$/CoTMPP nanosheets in the dark for positive and negative gate biases. The solid lines show the drain current vs gate voltage for various $V_{DS}$, and the open symbols show the square root of drain current (right vertical axis).

characteristics of the transistor. The measurements were performed under $N_2$ at room temperature in the dark after annealing at 373 K.

The characteristic V-shape transfer curves with one arm indicating electron transport (n-type) and the other indicating hole transport (p-type) were observed for the $C_{60}$/CoTMPP nanosheet-based FETs. This is in sharp contrast with earlier reported observations on $C_{60}$ nanowhisker based FETs that showed only n-type behavior.[25,28] The electron and hole mobilities calculated from Figure 5 are relatively low and on the order of $10^{-5}$ and $10^{-6}$ $cm^2$ $V^{-1}$ $s^{-1}$, respectively. Despite this, we believe that further device optimization could lead to higher


dx.doi.org/10.1021/ja211951v | *J. Am. Chem. Soc.* 2012, 134, 7204−7206

carrier mobilities. In this regard, it should be noted that the mobilities were calculated assuming a complete coverage of the channel, a situation that is clearly not achieved. As a result, these values represent a lower limit for hole and electron mobilities within the nanosheet.

Recently, the crystal structure of CoTMPP·$C_{60}$ (1:1) (zigzag chain of $C_{60}$ spheres with van der Waals "caps" of CoTMPP) was reported by Konarev et al.[27] The CoTMPP is located between two $C_{60}$ molecules while forming zigzag chains. It could therefore be argued that the zigzag chains of $C_{60}$ spheres and CoTMPP are responsible for the balanced electron/hole transport observed in our nanosheets.

It is well-known that $C_{60}$–porphyrin dyads undergo electron transfer under optical excitation.[29] To investigate whether such a process occurs within the $C_{60}$/CoTMPP nanosheets, we have remeasured the transistor characteristics while the devices were illuminated with visible light (see Supporting Information). Interestingly, all $C_{60}$/CoTMPP nanosheet-based FETs are found to be photoresponsive, although the sensitivity is not high. One possible reason for this could be the fast excited-state deactivation of porphyrin by the efficient spin–orbit coupling.[30]

In conclusion, we have successfully constructed supramolecular nanoarchitectures (nanosheets) comprising 1:1 $C_{60}$/CoTMPP by a simple LLIP method. The $C_{60}$/CoTMPP nanosheets exhibit ambipolar transport characteristics with nearly balanced hole/electron mobilities. The present results show that single co-crystals containing suitable D–A molecules can be made ambipolar, an important characteristic that could potentially be used to develop improved materials and devices. Importantly, the preparation of these nanosheets is very simple and can be applied not only to fullerenes, but also to other carbon-based materials. The successful preparation of hybrid nanoarchitectures with unique electronic characteristics by this very simple co-crystallization method can be viewed as an important stepping-stone to the fabrication of novel nanoscale devices.

## ■ ASSOCIATED CONTENT

### Ⓢ Supporting Information

Experimental detail; AFM image, Raman spectra of $C_{60}$/CoTMPP nanosheets; optical microscope images of $C_{60}$/CoTMPP nanosheets FET; transfer characteristics of $C_{60}$/CoTMPP FETs under red light illumination . This material is available free of charge via the Internet at http://pubs.acs.org.

## ■ AUTHOR INFORMATION


### Corresponding Author

Wakahara.takatsugu@nims.go.jp; D.Bradley@imperial.ac.uk; Thomas.anthopoulos@imperial.ac.uk


### Notes

The authors declare no competing financial interest.

## ■ ACKNOWLEDGMENTS


Part of this research was financially supported by a Grant-in-Aid for Scientific Research from the Ministry of Education and Culture, Sports, Science and Technology, Japan.


## ■ REFERENCES


(1) Kim, F. S.; Ren, G. Q.; Jenekhe, S. A. *Chem. Mater.* **2011**, *23*, 682–732.
(2) Zang, L.; Che, Y.; Moore, J. S. *Acc. Chem. Res.* **2008**, *41*, 1596–1608.
(3) Zhao, Y. S.; Fu, H.; Peng, A.; Ma, Y.; Liao, Q.; Yao, J. *Acc. Chem. Res.* **2010**, *43*, 409–418.
(4) Zaumseil, J.; Sirringhaus, H. *Chem. Rev.* **2007**, *107*, 1296–1323.
(5) Li, R.; Jiang, L.; Meng, Q.; Gao, J.; Li, H.; Tang, Q.; He, M.; Hu, W.; Liu, Y.; Zhu, D. *Adv. Mater.* **2009**, *21*, 4492–4495.
(6) Di Maria, F.; Olivelli, P.; Gazzano, M.; Zanelli, A.; Biasiucci, M.; Gigli, G.; Gentili, D.; D'Angelo, P.; Cavallini, M.; Barbarella, G. *J. Am. Chem. Soc.* **2011**, *133*, 8654–8661.
(7) Anthopoulos, T. D.; Setayesh, S.; Smits, E.; Colle, M.; Cantatore, E.; de Boer, B.; Blom, P. W. M.; de Leeuw, D. M. *Adv. Mater.* **2006**, *18*, 1900–1904.
(8) Zaumseil, J.; Friend, R. H.; Sirringhaus, H. *Nat. Mater.* **2006**, *5*, 69–74.
(9) Anthopoulos, T. D. *Appl. Phys. Lett.* **2007**, *91*, 113513.
(10) Mativetsky, J. M.; Kastler, M.; Savage, R. C.; Gentilini, D.; Palma, M.; Pisula, W.; Muellen, K.; Samori, P. *Adv. Funct. Mater.* **2009**, *19*, 2486–2494.
(11) Hizume, Y.; Tashiro, K.; Charvet, R.; Yamamoto, Y.; Saeki, A.; Seki, S.; Aida, T. *J. Am. Chem. Soc.* **2010**, *132*, 6628–6629.
(12) Konarev, D. V.; Lyubovskaya, R. N.; Drichko, N. V.; Yudanova, E. I.; Shul'ga, Y. M.; Litvinov, A. L.; Semkin, V. N.; Tarasov, B. P. *J. Mater. Chem.* **2000**, *10*, 803–818.
(13) Sawamura, M.; Kuninobu, Y.; Toganoh, M.; Matsuo, Y.; Yamanaka, M.; Nakamura, E. *J. Am. Chem. Soc.* **2002**, *124*, 9354–9355.
(14) Moriyama, H.; Kobayashi, H.; Kobayashi, A.; Watanabe, T. *Chem. Phys. Lett.* **1995**, *238*, 116–121.
(15) Konarev, D. V.; Khasanov, S. S.; Otsuka, A.; Saito, G.; Lyubovskaya, R. N. *Chem.—Eur. J.* **2006**, *12*, 5225–5230.
(16) Stephens, P. W.; Cox, D.; Lauher, J. W.; Mihaly, L.; Wiley, J. B.; Allemand, P. M.; Hirsch, A.; Holczer, K.; Li, Q.; Thompson, J. D.; Wudl, F. *Nature* **1992**, *355*, 331–332.
(17) Wakahara, T.; Sathish, M.; Miyazawa, K. i.; Hu, C.; Tateyama, Y.; Nemoto, Y.; Sasaki, T.; Ito, O. *J. Am. Chem. Soc.* **2009**, *131*, 9940–9944.
(18) Mohnani, S.; Bonifazi, D. *Coord. Chem. Rev.* **2010**, *254*, 2342–2362.
(19) Zhang, X.; Takeuchi, M. *Angew. Chem., Int. Ed.* **2009**, *48*, 9646–9651.
(20) Boyd, P. D. W.; Reed, C. A. *Acc. Chem. Res.* **2005**, *38*, 235–242.
(21) Tashiro, K.; Aida, T. *Chem. Soc. Rev.* **2007**, *36*, 189–197.
(22) Sgobba, V.; Giancane, G.; Conoci, S.; Casilli, S.; Ricciardi, G.; Guldi, D. M.; Prato, M.; Valli, L. *J. Am. Chem. Soc.* **2007**, *129*, 3148–3156.
(23) Nobukuni, H.; Tani, F.; Shimazaki, Y.; Naruta, Y.; Ohkubo, K.; Nakanishi, T.; Kojima, T.; Fukuzumi, S.; Seki, S. *J. Phys. Chem. C* **2009**, *113*, 19694–19699.
(24) Sato, S.; Nikawa, H.; Seki, S.; Wang, L.; Luo, G.; Lu, J.; Haranaka, M.; Tsuchiya, T.; Nagase, S.; Akasaka, T. *Angew. Chem., Int. Ed.* **2012**, *51*, 1589–1591.
(25) Doi, T.; Koyama, K.; Chiba, Y.; Tsuji, H.; Ueno, M.; Chen, S. R.; Aoki, N.; Bird, J. P.; Ochiai, Y. *Jpn. J. Appl. Phys.* **2010**, *49*, 04DN12.
(26) Anthopoulos, T. D.; Singh, B.; Marjanovic, N.; Sariciftci, N. S.; Ramil, A. M.; Sitter, H.; Colle, M.; de Leeuw, D. M. *Appl. Phys. Lett.* **2006**, *89*, No. 213504.
(27) Konarev, D. V.; Kovalevsky, A. Y.; Li, X.; Neretin, I. S.; Litvinov, A. L.; Drichko, N. V.; Slovokhotov, Y. L.; Coppens, P.; Lyubovskaya, R. N. *Inorg. Chem.* **2002**, *41*, 3638–3646.
(28) Ogawa, K.; Kato, T.; Ikegami, A.; Tsuji, H.; Aoki, N.; Ochiai, Y.; Bird, J. P. *Appl. Phys. Lett.* **2006**, *88*, 112109.
(29) D'Souza, F.; Ito, O. *Chem. Soc. Rev.* **2012**, *41*, 86–96.
(30) Sutton, L. R.; Scheloske, M.; Pirner, K. S.; Hirsch, A.; Guldi, D. M.; Gisselbrecht, J. P. *J. Am. Chem. Soc.* **2004**, *126*, 10370–10381.